TRANSPARENT AMORPHOUS SILICON SENSORS FOR THE ALIGNMENT SYSTEM OF PARTICLE DETECTORS

Marcos G. Fernández
CIEMAT
Avda. Complutense, 22
28040 Madrid (Spain)

1. INTRODUCTION

In CMS resolutions from 5 to 20% for 1 TeV muons (up to η=2.4) will demand position accuracy of the muon spectrometers with respect to the tracker detector comparable to the muon chambers resolution (100 μm). With a 4T magnetic field, stability of the muon chambers at the 100 μm level is not guaranteed during detector operation. In fact, due to the magnetic forces affecting the return yoke, motions from a few mm to 1-2 cm are expected [1]. Therefore the muon chambers position needs to be monitored, at any time, with respect to the tracker with the maximum possible accuracy. This is the role of the CMS alignment system [2]. In order to minimise the interference with the rest of subdetectors a solution based in transparent sensors sharing a common laser line has been adopted. The selected optical sensors, in addition to the required accuracy, have to be radiation hard and need to have large sensitive area.

In ATLAS, the momentum measurement in the muon spectrometer demands a precision of the order of 10% for muons of transverse momentum of 1 TeV [6]. The target level of accuracy for the precision chamber alignment is such that the alignment contribution to the final measurement error stays well below the intrinsic precision chamber measurement error (100 μm).

The baseline for the alignment system in both experiments are the transparent amorphous silicon detectors [3], or ALMY sensors. They were designed with the aim of providing position resolutions of the order of 1 μm over a sensitive area of 2×2 cm^2.

There are two types of ALMY sensors: based on crystalline silicon or amorphous silicon (a-Si) as the active material. The latter may be constructed using a single a-Si layer, called Schottky sensors, or using three a-Si layers: p-doped, intrinsic and n-doped, called p-i-n.

In this document we will present a historical review of ALMY sensors. The starting point was 1993 when the first prototypes were built. A description of their performance at this early stage will make clear which features have to be modified in order to cope with the stringent requirements imposed by ATLAS and CMS. As time went by, the problems were fixed and nowadays a fine working and operational ALMY sensor has been built. The following sections of this paper show how these aims were achieved. In section 2 the reader will know where and when ALMY sensors were born. It explains some reasons why amorphous silicon was chosen as photosensitive material. Section 3 intends to describe the morphology and physical properties of this device. Next sections

present results from the diverse characterisations from ATLAS and CMS. Particularly, section 4 deals with the uniformity and spatial resolution of the first prototypes. Details on the light transmission after one sensor are given in section 5. The different radiation hardness tests for ALMYs are introduced in section 6. The propagation of a plane wave through the different layers helps to understand the origin of the systematics found in the first prototypes (section 7). The performance of the new ALMY sensors is presented in section 8.

This paper should be considered as a product of the collaboration between the CMS and ATLAS communities. Particularly, from CMS, CIEMAT Madrid and the University of Cantabria (UC), Santander. In the ATLAS side, the Max Plank Institute (MPI) from Munich.

2. A BIT OF HISTORY

The ancestor of the current ALMY[1] sensors were crystalline strip sensors devised by W. Blum et col [3] at MPI. These sensors were produced by CSEM at Neuchâtel. Crystalline silicon (c-Si) was used as active material to work on the principle of silicon strip photodiodes. Sensors based on c-Si were transparent for infrared light. They had 67 strips along one direction (for the ATLAS muon spectrometer the highest precision is needed only in one coordinate) over an area of 20×20 mm^2. The beam spot position along the preferred direction was determined as the centre-of-gravity of the incoming Gaussian beam. Non uniformity of the strip response accounted for sensitivity variations to about 5%. The non linearity error associated was in the range of 10-20 μm. By measuring the deviations in an automated laser scan of the sensor surface and then interpolating between measurements, a position resolution of 2 μm was achieved [3]. The second coordinate measurement was provided by current division on the strips, since they were read out at both ends [4]. Due to fluctuations in the strip resistivity, its resolution was limited about 25 μm. The resolution degraded near the edges of the sensor.

Spreads in the beam deflection (after traversing the sensor) between 10 and 25 μrad for maximum deflections of about 200 μrad were observed. Using the same method as above, the beam deflections could be corrected to 1-1.5 μrad by precalibration.

The lack of uniformity in the response due to those variations in the strip sensitivity, the degradation near the edges and the expected higher damage produced by radiation on crystalline structures led to discard the crystalline technology against the technique based on *amorphous* silicon.

It was H. KROHA the first one to propose amorphous silicon as active material for the ALMY sensors. In contrast to crystalline, amorphous silicon films are fully active and position resolutions could be improved due to the better homogeneity. Besides that, strips were photolithographied in both directions, thus improving resolution in the transversal coordinate. Films of amorphous silicon are transparent for visible light emitted by semiconductor laser diodes.

[1] ALMY stands for ALigment of MYon chambers

3.- AMORPHOUS SILICON STRIP SENSORS

Amorphous silicon sensors consist of a thin film of hydrogenated amorphous silicon (a-Si:H) deposited between two layers of indium-tin oxide (ITO) electrodes on a glass substrate. The hydrogen concentration, controlled by the process temperature, is essential for the electrical and optical properties of the sensors. In reference [5] it is found that the H content in the thin film shifts the absorption edge to shorter wavelengths and causes a decrease of the density.

A sketch of the sensor can be seen Figure 1. When the a-Si:H thickness is 0.5 μm, we will refer to type I sensors. Type II sensors have 1 μm of photosensitive material. The sensor layers are deposited with Chemical Vapour Deposition (CVD) techniques on an about 0.5 mm thick glass substrate. Upper and bottom ITO layers (50-100 nm thick) are deposited and then structured orthogonal using photolithographic methods. A complete description of the main characteristics of both types of sensors is found in [6].

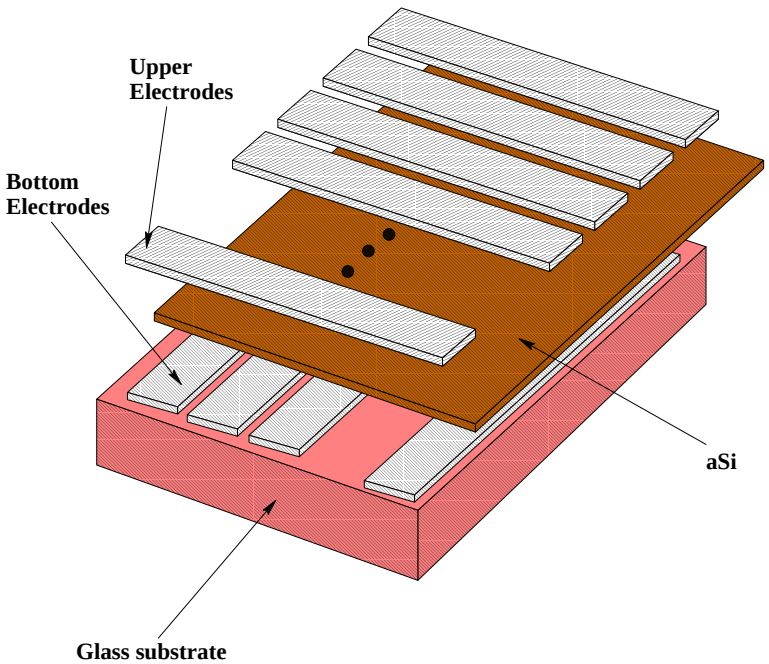

Figure 1 – 3D pictorial view of an ALMY sensor.

Three different versions of the readout electronics have been used. In all cases the photocurrents on the strips are multiplexed, amplified by a common current voltage transformer, digitised and stored in a local memory. Commercial sensors [7] were delivered with an electronics box ready to connect to the RS232 cable. Prototypes tested at MPI were addressed via a custom designed VME interface board and lately using a serial line without degradation of speed.

The signal on the sensor is fitted to a Gaussian, since lasers coupled to monomode fibers are used. Pointing stability of the different sources may require averaging over about a dozen of measurements. Noise from the detector and electronics is negligible even for long unscreened cables [8].

An in-depth study of the performances of the sensors relies on surface scans over about 80% of the sensor area. Therefore, sensors are mounted on XY computer controlled

tables. The scan provides information on the spatial uniformity of the sensor, by comparing the reconstructed motion against the displacement of the platforms (with resolutions better than 2 μm). The transmitted beam is recorded and compared with the undeflected beam providing an estimation of the beam deflection and the transmittance ratio.

Regarding the transmittance, type I sensors are 80% transparent for 690 nm while 90% of the incoming light is transmitted for 780 nm. Sensitivity is higher for type I sensors (0.1 A/W), since absorption in the a-Si:H increases for shorter wavelengths.

Next two sections will describe these points in detail. We are about to show a summary of the observed features of the sensors. Two different samples of sensors with amorphous silicon as active material have been used. First one is made of old prototypes. Second sample implements corrections for the problems found in the first sample. A summary of the identity of the sensors and the test is given in Table 1.

Table 1: Sets of sensors presented in this work. Reports of the individual test are found in references [3],[9],[10-13] for ATLAS and [8], [14,15,16,17] for CMS.

	No. of sensors	Tested by
Sample 1	117 + 7	ATLAS + CMS
Sample 2	27	ATLAS & CMS

First subset contains 117 sensors (about half of type I and half of type II), tested at MPI for ATLAS plus 7 commercial sensors characterised for CMS at the laboratories of the University of Cantabria. Second sample is made of 27 (type II) new sensors and will not be mentioned until they are introduced in section 8. Special mention should be done on the sources used in both laboratories. While MPI used diode lasers at 690 nm (for type I sensors) and 780 nm (for type II sensors), CIEMAT/UC used two HeNe (632.8 nm) and one laser diode (686 nm).

4. LINEARITY AND SENSOR UNIFORMITY

Linearity measurements indicate how well the displacements of the light spot are reconstructed by the sensor. It also shows the minimum displacement that the sensor can resolve. During a scan, the difference between the real and the reconstructed displacement allows to determine the spatial uniformity of the sensor. The lack of uniformity represents a systematic error on further measurements.

The scans may be done along one line on the sensors. While the laser light is fixed, the sensor is moved by constant steps. After each step of the platform, the XY position of the spot on the sensor is determined performing a Gaussian fit on both coordinates. Afterwards, the reconstructed displacement is compared with the displacement of the platform. If the sensor were perfect, a slope of 1 should be found. In practice, the linearity differs slightly from the unity. Discarding any contribution from the stepping motor, the difference comes from unstability in the source (which, under normal operation, contributes as an statistical error), from angles in the mounting (the direction of the scan and the internal frame of the sensor are not perfectly aligned) and from eventual non-uniformities in the sensors.

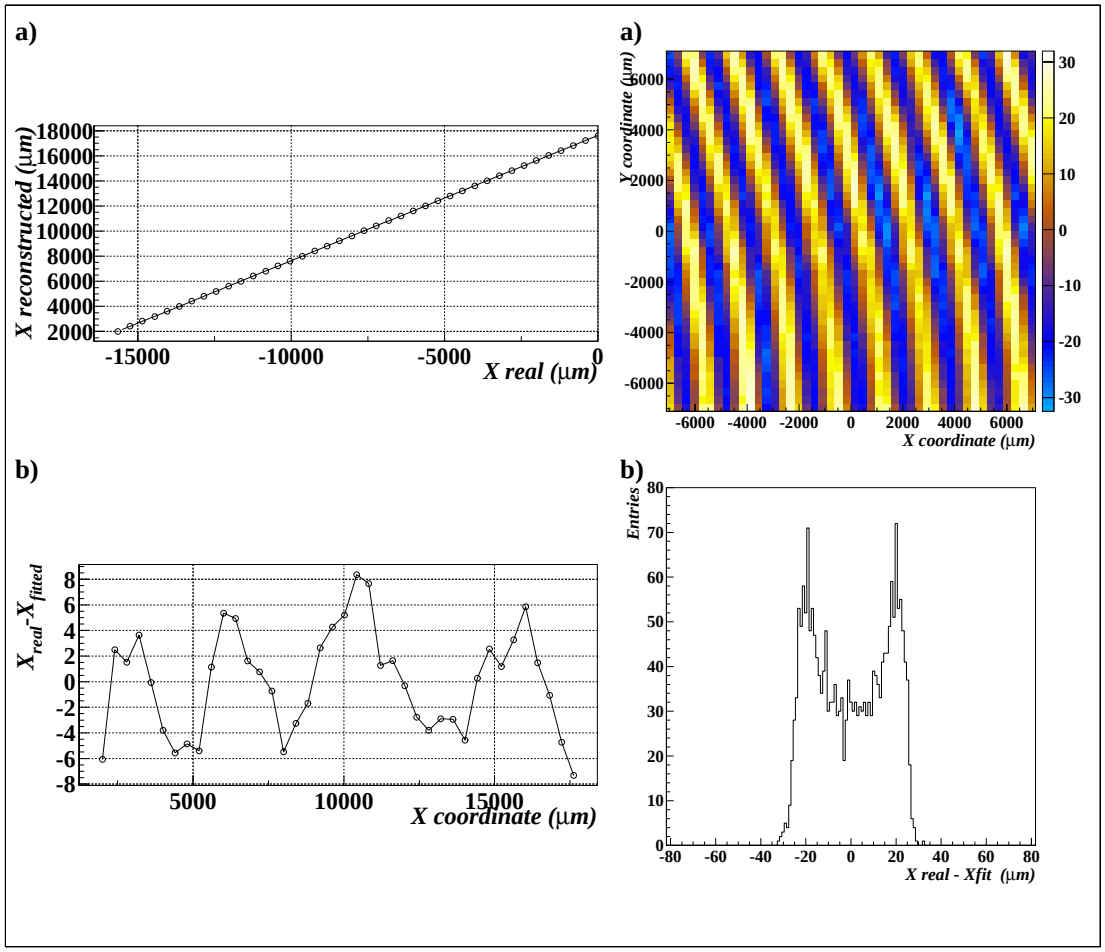

Figure 2 – a) Reconstructed position along a 1D scan of a sensor.
b) Residuals of the linear fit.

Figure 3 – a) Scan (312×312 μm^2) of one ALMY sensor type II b) Spatial resolution.

2a) shows the reconstructed beam position along one scan "parallel" to the horizontal strips (X direction in what follows). The residuals to the linear fit are shown 2b). It is clear from this figure that the residuals are not randomly distributed but follow a pattern. It was confirmed [8,9] that the pattern was intrinsic to the sensor (different for different sensors) and not homogeneous. In fact, similar patterns (but not correlated) were obtained for the integrated photocurrent response.

Extending the scan to the rest of the surface of the sensor, a 2D picture of the spatial inhomogeneity is obtained. 3a) is an example of this. Each entry in the plot is a value of the linearity residuals. A histogram of the residuals shows the distribution of those entries above (see 3b)). Gaussian shapes of these distributions would be desirable. It would mean that patterns, although exist, do not show huge systematics that spoil the Gaussian characteristic.

Fifty six sensors (out of 117 from MPI) [10] had a Gaussian resolution distribution. All 7 sensors from CIEMAT/UC had gaussian shape [17]. Regarding spatial uniformity, all sensors at MPI kept below 5 μm (Gaussian width obtained from the fit), while CIEMAT/UC studies obtained resolutions below 5 μm except for the measurements

done with a laser diode for the sensor coordinate perpendicular to gravity (very likely induced by a problem with the laser [17]).

5. BEAM TRANSMISSION

When light propagates in a medium it suffers interactions with matter thus, the light can change speed and direction depending on the traversed medium. In addition, part of the incoming energy is reflected in the interface of the media. When the light traverses layers of materials, interferences may appear due to the phase difference between the incoming and reflected light. Both effects, despite their very different origin, produce a beam distortion.

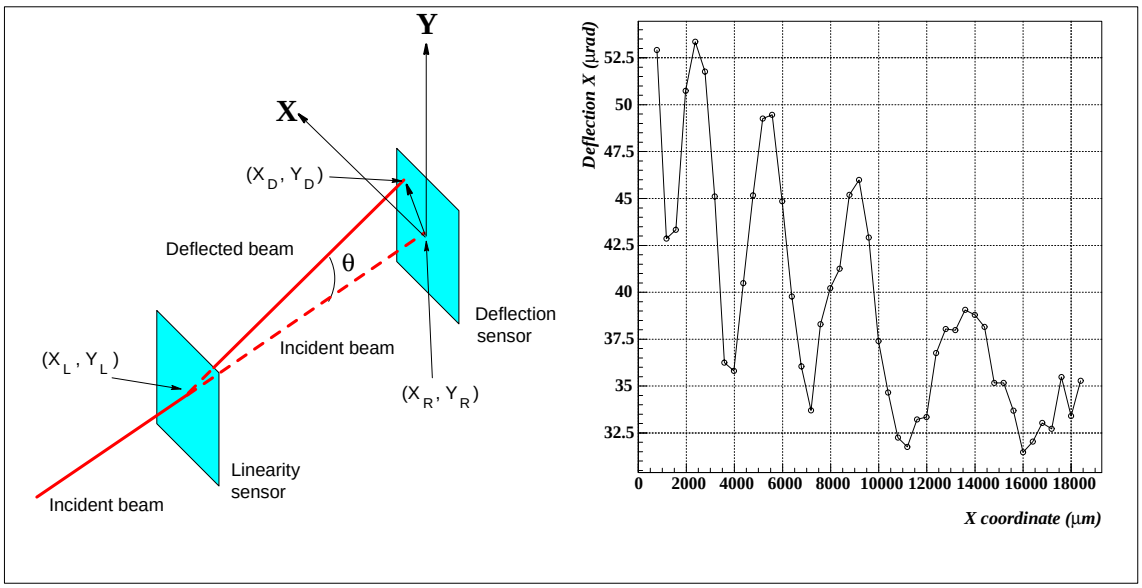

Figure 4 – Deflection measurement procedure.

Figure 5 – 1D scan along an horizontal line in the sensor. The slope and the oscillations are clearly seen.

Unless the sensor were a perfect planeparallel structure under normal incidence, the incoming beam would suffer a shift with respect to the original ray (non normal incidence on a planeparallel layer) and a change in direction (normal incidence on a non planeparallel layer). When studying the transmitted light (either using a CCD camera to collect the light or even another sensor), the position of the beam after a sensor differs from the original position of the laser spot. Both effects above will be present and the overall result will be interpreted here as a pure geometrical beam deflection.

The procedure to measure the beam deflection is sketched in Figure 4. The undeflected beam is recorded by the second detector when the first sensor is removed from the light path. Then, it is placed back and scanned with the laser beam. The light collected in the second detector will account for the beam deflection due to the presence of the first sensor. This method also allows to calculate the transmittance of the system by comparing the amount of light collected with the first sensor in the beam path, to the light collected without it.

The same systematic employed for the uniformity study may be employed here. A 1D scan of the sensor (see Figure 5) reveals that deflection angles distribute with an oscillating pattern along a slope. This characteristic behaviour is common to all sensors studied in the first sample. As explained in [8] and [15], the slope can be associated with a curvature of the substrate. The existence of an oscillating pattern could tempt to associate it with the patterns obtained for the uniformity (see Figure 2a)). However, there is not spatial correlation between both [15].

Surface scans of a sensor produce 2D deflection distributions depending on the position of the spot on the first sensor. One example is given in Figure 6. The magnitude of the deflection angle is easily computed from Figure 7.

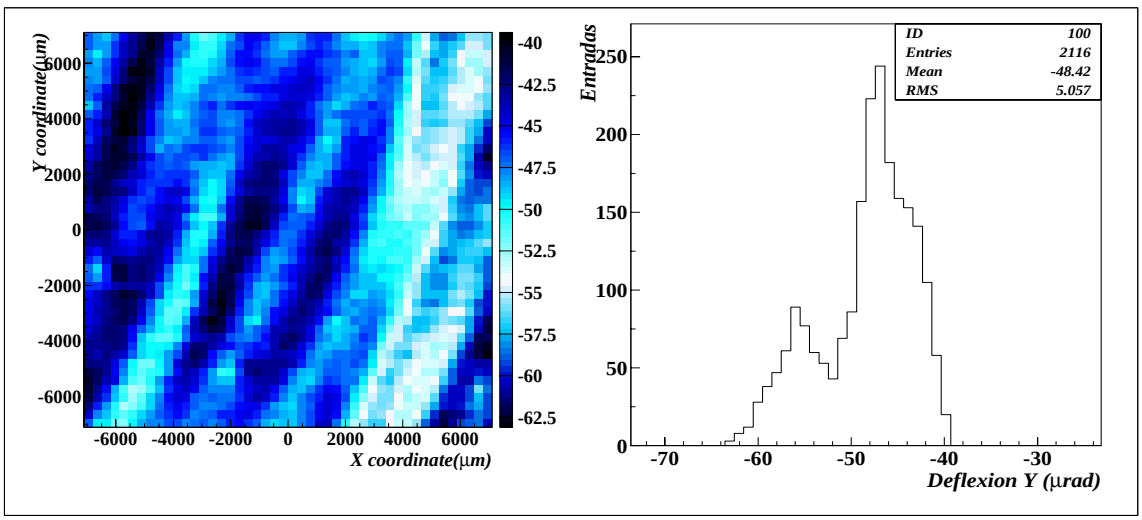

Figure 6 – Scan (312×312 μm^2) of one ALMY sensor type II, as seen by a CCD camera. The sensor shown is not that in Figure3.

Figure 7 – Distribution of the deflected angles.

Only one of the sensors of the first sample tested at MPI showed Gaussian deflection distributions with a width below 5 μrad [10]. One of the sensors from CIEMAT/UC had Gaussian deflection distributions, but the width was above 5 μrad. In general, the average values could range from a few μrad to hundreds of μrad. These values are above constraints for applications such as ATLAS and CMS alignment systems [2,6]. It means that, at this stage, the sensor deflection has to be corrected in order to be used.

An offline correction of the deflection angle can be accomplished by precalibration of the sensors. This precalibration makes sense only if they are stable in time. Reference [15] presents a correction of two scans of the same sensor delayed by one month in time. Deflection mean values are equal within 2 μrad with a spread below 3 μrad. Scaling of the transmitted beam is also needed. It means that the same calibration stands independently from the distance with respect to the first sensor. References [15] and [18] show that scaling is not hold when one the detector measuring transmission is closer than about 1 m. However, intercorrection of configurations under 2 and 3 m works fine [17]. As it was already pointed out in [15], it could well happen that deflection and diffraction processes affect in the near field, and seem to have less importance at distances larger than 2 m. New measurements on this topic are planned.

The absorption of the a-Si:H decreases very fast for short wavelengths. In fact, transmission ratios as low as 22% were obtained for HeNe lasers [15]. Transmittance increases to 80% for 690 nm in type I sensors [6]. Type II sensors are more transparent under 780 nm and reach almost 90% in transmittance. As it will be explained in section 7, sensors can still be optimised for maximum transmittance.

6. IRRADIATION

In CMS, some of the sensors located at $|\eta|\approx 3$ will undergo gamma irradiation as high as 1 Mrad/year, neutron fluences up to 10^{14} per cm^2 and year and about 10^{13} charged hadron fluences (mainly pions) per cm^2 and year. In the ATLAS side, the hottest spot for the muon spectrometer (E1 layer) will be $1.5\cdot10^{12}$ neutrons/cm^2 and $2\cdot10^{14}$ neutrons/cm^2 per year for the inner detector. The choice of amorphous silicon sensors has been favoured by the expected better resistance of this material to radiation.

ATLAS has made several irradiation tests on ALMYs. First one took place at the ISIS spallation source at the Rutherford Laboratory. Amorphous silicon sensors and Corning 1 glass substrates were irradiated with doses of $(1\text{-}2)\times10^{14}$ neutrons/cm^2 below 10 keV and $(0.5\text{-}1)\times10^{14}$ neutrons/cm^2 above 10 keV. No degradation of the transmission ratios and glass substrates were observed [6]. The sensors were not powered during this test. Two more tests were performed, this time in PROSPERO (Dijon, France). PROSPERO is a research reactor that provides neutrons ($0.7\text{-}1.5\times10^{14}$ total fluence, energies between 0.73 and 0.77 MeV) and gammas. During the first test, Schottky diodes and Corning 1 glass were irradiated, this time with readout electronics but switched off. Sensors were measured and no change in transmission and sensitivity was found up to $(0.5\text{-}1)\times10^{11}$ neutrons/cm^2 [19]. Second one included a full operating setup made of 4 *new* sensors (see section 8) with different operational amplifiers and a laser rigidly fixed to a portable bench. Sensors and laser were operational up to the maximum dose of 10^{13} neutrons/cm^2. The sensors and laser continued working without problems after the test [20].

CMS irradiated [21] two different sensors with gamma rays and neutrons. One of the sensors having a unique a-Si:H layer (commercial Schottky sensor) equipped with front-end electronics[2], and a second one constructed with three a-Si layers (p-i-n prototype sensor) on the substrate plate. Sensors were irradiated with gamma rays and with neutrons, independently but consecutively. Gamma irradiation was done, in several steps, with gamma rays from ^{60}Co sources at the NAYADE facility at CIEMAT (Madrid, Spain). The total dose is the equivalent to 10 years of CMS operation (10 Mrad). Neutron irradiation was done, in one go, using the fast neutron source based on the MGC-20 cyclotron facility available at ATOMKI (Debrecen, Hungary). The mean neutron energy of this source was 3.7 MeV and the total fluence amounted. The multiplexors died after an accumulated dose of 20 krad gammas. However resistors and capacitors were still alive after gammas and neutrons irradiation [21,22]. No variation on the deflection angle spreads were observed. A complete study of the transmission using an Perking-Elmer Lambda 9 spectrometer does not allow to detect any degradation in the visible spectrum [23].

[2] Mainly multiplexors, resistors and capacitors

7. ALMY SIMULATION

The systematic variations observed in the spatial uniformity, transmission and sensitivity were remarkably regular across the sensor surface. It might well happen that local differences in the thickness of the a-Si:H layer could lead to a non homogeneous response across the sensor. It was believed that these periodic thickness variations could be caused by resonant effects in the plasma CVD apparatus. A solution to the problem would come from an improvement to the system [13].

A more detailed analysis [10] showed that the relative variations of the transmittance between sensors should directly correspond to relative differences in the measured absorption. However measured variations were smaller than expected. Absorption alone could not explain this data. Therefore, the light reflected in the different layers was playing a role in the observed oscillations. If there was light going back and forth, then very likely there were interferences in the sensor.

A rigorous demonstration of this hypothesis needs a simulation of the propagation of a plane wave through the sensor (taking into account all the internal reflections in the several layers). A full description of the simulation process [25] and theory of the multilayers [26] escapes the scope of this paper. Only the most important results will be presented here. The input for the simulation are photometric measurements of transmittance (T) and/or reflectance (R) spectra of the layers that conform an ALMY. Only refraction indexes[3] *(n,k)* in a narrow wavelength range were known for the a-Si:H. For the rest of layers, information of *(n,k)* was given only at four wavelengths. The purpose is to reproduce the T and R spectrums for a Schottky type ALMY. The single layer measurements of T were done by JENOPTIK [24] on a pin-type sensor. The measurement of T for the Schottky-type sensor was done at CIDA [23].

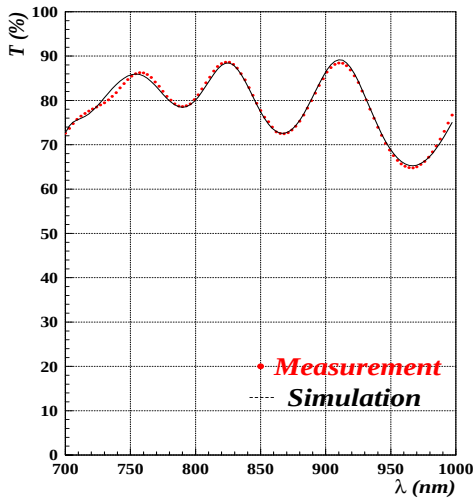

Figure 8 – Transmittance for the system ITO + a-Si:H + ITO + glass substrate. The effect of a finite size substrate is also included as in Figure 8.

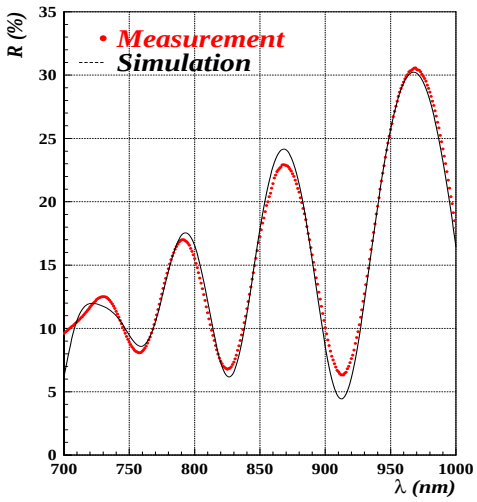

Figure 9 – Reflectance for the same system as in Figure 8.

[3] Absorbing media as metals or semiconductors are described by a complex refraction index ñ = n-ik.

Due to the reduced amount of data available, the simulation sets free the three unknown parameters of the film (n, k and d –the thickness–) until the difference between the measured T and/or R and those simulated is a minimum. There are physical constraints imposed on the indexes and estimations of the layer thickness that help to reduce the number of solutions of the system. Therefore, each layer is simulated independently and finally the simulation of an ALMY is done using the data obtained from the individual layers as input. In Figure 8 and Figure 9. we show the result for the whole ALMY sensor. The continuous line correspond to the simulation, while the points are the measured values. Figure 10 gives the output *(n,k)* indexes obtained from the simulation. The agreement in the real index is very good. The simulation is found to be very sensible to changes in *k*. On the other hand, it has been experimentally shown that differences in the *k* value, as those observed between simulation and the measurement are obtained even for two measurements in the same layer [24]. In fact, the optical properties of the a-Si depends strongly on the preparation conditions and on the doping with hydrogen.

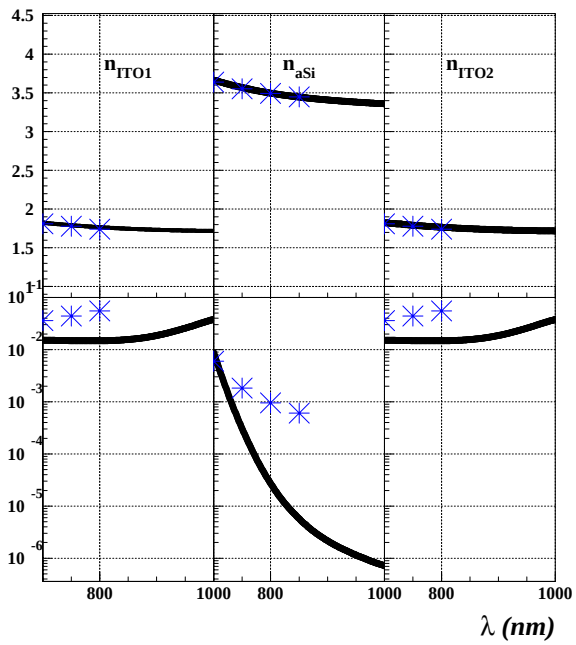

Figure 10 – Real and imaginary components of the refraction index of ITO (upper electrodes), a-Si:H and ITO (bottom electrodes). Asterisk are the mono-layer starting values for the simulation. The line represents the calculated value. The set of *(n,k)* shown here reproduce T and R as shown in Figure 8 and Figure 9.

This simulation validates the hypothesis of interferences in the several layers of the system. In addition, it is a useful tool in order to make an optimisation of the ALMY sensors for maximum transmission and to study the tolerance in the construction process for such maximum to be achieved.

8. THE NEW SENSORS

Section 7 showed how interferences in the various layers of material reproduce the T and R spectrum measurements. A suitable antireflection coating was designed by

JENOPTIK and first prototypes coated in the backside of the substrate were built. These prototypes have been now extensively tested.

Twenty seven sensors have been tested at MPI. These sensors are amorphous silicon sensors type II (see section 3). Sensors are coated after the ITO and a-Si:H layers are deposited on the substrate before bounding. Then the sensor is placed in the ceramic frame, bounded and glued to it. The electronic board is removable, so it can be replaced, if necessary, without damaging the sensor.

The sensors were read out with VME and serial bus interfaces producing the same results. Readout speed of serial line is 10 Hz. One hundred and twenty eight sensors can be readout using a standard PCI-RS232 interface. The final step of the electronics readout system will be to use the CAN bus [27], since it has been chosen as the standard for the LHC Detector Control System.

The improvement obtained by the antireflection coating can be deduced by inspection of Figure 11. First row contains spatial uniformity for both coordinates of the sensor. Next row shows deflection angle[4] distributions and last row contains the photoresponse of the sensor (in ADC counts) and the transmittance. The lack of patterns is immediately observed. The same result applies for all the rest of the scanned sensors. As a kind of summary we present in Figure 12 the performance of all the studied sensors. It summarises (from top to bottom): spatial uniformity for both coordinates, angular resolution and transmittance as a function of the sensor number (the number used is just for identification purposes). The gap between sensor #16 and #24 corresponds to a set of uncoated sensors. Mean values of angular and spatial resolutions fall below 5 μrad and 5 μm, respectively. These values are within the specifications for CMS and ATLAS alignment systems. As it is pointed out in section 7, these performances can be still optimised.

Although it has not been mentioned in the former sections, and as a common characteristic of all the detectors implementing a-Si:H as active material, the old ALMY prototypes presented an ageing problem. Ageing of a-Si is known since 1977 as the Staebler-Wronski effect [28] consisting in an increase of the number of traps for the charge carriers. The density of these states increases with the illumination time and the light intensity. The natural solution adopted was a reduction of the laser power which required a modification of the electronic amplification to increase the signal height without increasing the noise. The result is that after 500 hours (twice ATLAS and CMS estimated alignment measurement time) of continuous illumination of four ALMY sensors at nominal working power, the photoresponse only decreased by 3% which means a systematic distortion below 5 μm in the position.

[4] The distributions of the deflection angles have been fitted to a plane to eliminate the contribution of the glass thickness.

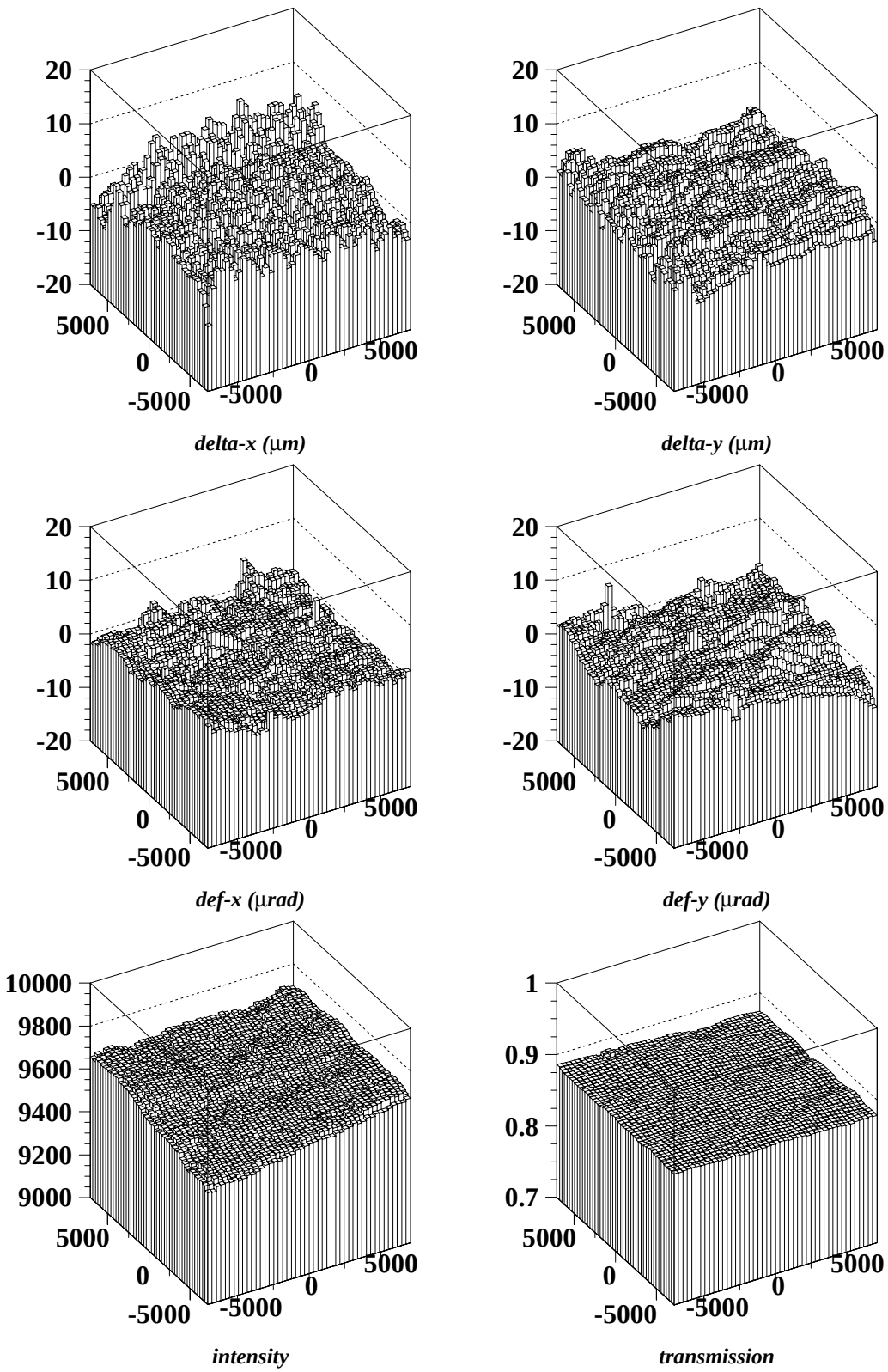

Figure 11 – Performance of the new ALMY type II sensor. From top to bottom, left to right: spatial uniformity X, spatial uniformity Y, X and Y deflection distributions, integrated photocurrent and transmittance.

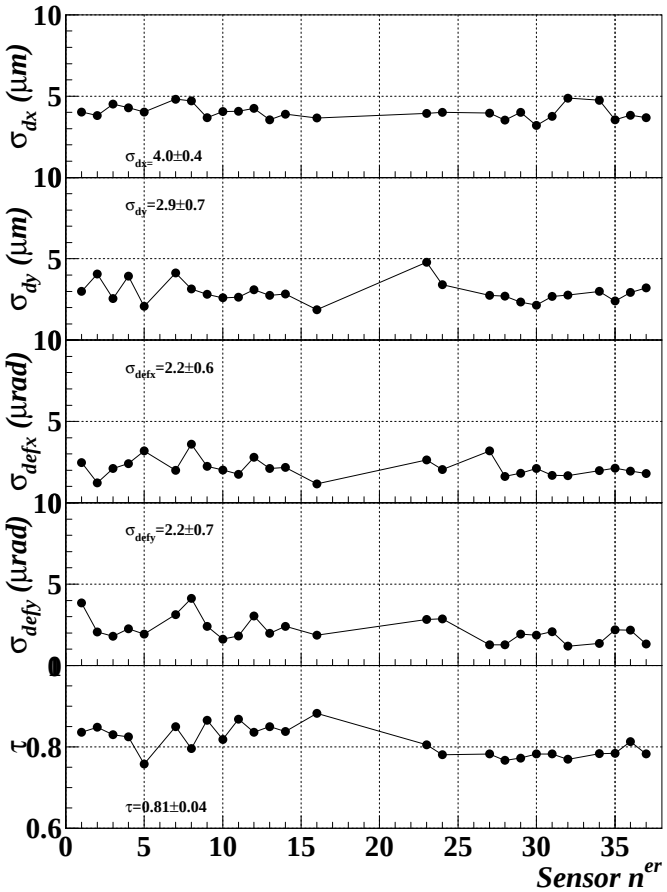

Figure 12 – ALMY performance for 27 sensors with coating (all available in July 99).

9. SUMMARY AND CONCLUSIONS

ALMY sensors were born as a solution for the alignment of extended structures where large dynamic ranges and special hardness conditions were needed. ALMY sensors provide a novel method for light detection. The sensor itself detects and transmits the light with minimal distortion, providing an absolute reference. Even at the early stage of development, other applications, with less demanding requirements than high energy physics detectors, could benefit of ALMY features. ALMY sensors can be built custom designed, since size is not handicap for uniformity. Radiation hardness and insensibility to magnetic fields make them very appealing for other areas as space or civil research.

Amorphous silicon sensors have proven to be radiation resistant up to 10^{14} n/cm^2 accumulated to 10 Mrad of gamma rays. The spatial resolution is better than 5 μm for all the sensors tested. The sensor non-uniformity does not show any systematic component. Traversing light is deviated after the sensor (this is common to any transparent medium) by a small (at the level of μrad) constant angle with an uncertainty below 5 μrad. Without any other improvement and loss in resolution, 10 sensors can be aligned with the same beam. ALMY sensors have a long time stability and no major ageing effects. The ALMY sensors fulfil the requirements of the applications for which were initially developed.

ALMY sensors are near the final development stage. Transmittance optimisations by means of a proper election of layer thickness is still missing. A maximum transmittance of 96 % can be achieved attending the simulations. CAN bus interface is currently being done and only tests of new sensors after mass production is needed.

10. ACKNOWLEDGEMENTS

It is my pleasure to thank my colleagues from CIEMAT (Dr. A. Ferrando, A. Molinero and J.C. Oller), from the University of Cantabria (Prof. T. Rodrigo, C.F. Figueroa, N. García, I. Vila, A. L. Virto, Dr. P. Arce and Dr. F. Matorras). In Germany, I am thankful to Prof. Dr. V. Soergel for supporting part of this job at MPI. I am indebt to Dr. Stefan Schael, Dr. H. Kroha, Dr. V Danielyan, Dr. R. Richter, Dr. A. Ostapchuk, S. Chouridou and S. Horvat.

12.- REFERENCES

[1] The CMS Collaboration, “The Muon Project. Technical Design Report”, CERN/LHCC 97-32, CMS TDR 3, 15 December 1997.
[2] The CMS Collaboration, “The Compact Muon Solenid Technical Proposal”. CERN/LHCC94-38, 15 December 1994.
[3] W. Blum et al, *Nucl. Instr. and Meth.A* 367 (1995) 413-417
[4] See H. Kroha, ALMY Workshop, MPI Munich, 6-8 April 1998
(http://wwwatlas.mppmu.mpg.de/mdt/library/alignment_workshop.html)
[5] E. C. Freeman and W. Paul, *Phys. Rev. B* **20**, 716 (1979)
[6] The ATLAS Collaboration,”The Muon Spectrometer Technical Design Report”, CERN/LHCC 97-22
[7] EG&G Heimann Optoelectronics, P. O. Box 3007, 65020 Wiesbaden, Germany
[8] J. Berdugo *et al*, *Nucl. Instr. and Meth.A* 425 (1999) 469-479
[9] Volker Bartheld, MPI-PhE/ 97-04
[10] S. Schael, ALMY Workshop, MPI Munich, 6-8 April 1998
http://pcatlas3.mppmu.mpg.de/~schael/almy/almy_mpi_april98.pdf.gz
[11] W. Blum, *et al*, *Nucl. Instr. and Meth.A* 377 (1996) 404-408
[12] W. Blum, *et al*, IEE Transactions on Nuclear Science, Vol. 43, No. 3, June 1996
[13] H. Kroha, *Nucl. Phys.B* (Proc. Suppl.) 54B (1997) 80-85
[14] M.G. Fernández, ALMY Workshop, MPI Munich, 6-8 April 1998
[15] M. G. Fernández *et al*, CIEMAT 1999/890 and, *Nucl. Instr. and Meth.A (in press)*
[16] David P. Eartly and Robert H. Lee, CMS NOTE 1998/004
[17] M. G. Fernández , Graduation thesis (CMS 1998-124 / THESIS) (in Spanish)
(http://cmsdoc.cern.ch/documents/98/dec1998_124.ps.Z)
[18] S. Horvat and S. Schael, “Tests of ALMY I Sensors”, August 6, 1999
(http://pcatlas3.mppmu.mpg.de/~schael/almy/test_of_ALMY.ps.gz)
[19] H. Kroha (private communication)
[20] S. Schael, MDT meeting, CERN June 1999
(http://pcatlas3.mppmu.mpg.de/~schael/almy/almy_cern_june99.pdf.gz)
[21] M. G. Fernández et al.,”Gamma irradiation of semitransparent amorphous silicon sensors”, *Nucl. Instr. and Meth.A (in press)*
[22] J. Cárabe *et al.*, CIEMAT note (in preparation).
[23] CIDA, Research & Engineering Departments. Arturo Soria, 289. 28033 Madrid (Spain).
[24] JENOPTIK Laser, Optik, Systeme GmbH, Prüssingstr. 41, 07745 Jena (Germany).
[25] A presentation of the whole simulation can be downloaded from
http://wwwae.ciemat.es/~mfg/2D/almystatus_MPI_100599.ps.gz. A paper is in preparation.
[26] Max Born, Emil Wolf “Principles of Optics”, Pergamon Press 1959
[27] Varuzhan Danielyan, Stefan Schael “Proposal for a new Readout for MPI-ALMY Detectors”, ALICE/98-51, ATLAS ATL-COM-MUON-98-028, 9 November 1998
[28] M. Stutzmann, W. B. Jackson, and C. C. Tsai, Physical Review B Volume 32, Number 1 1 July 1985